SUPPLEMENTARY MATERIALS AND METHODS

Animals

Mice were maintained in standard conditions with food and water ad libitum. All animal procedures were approved by local committees, in accordance with the European Communities Council Directive (86/609/EU). B6CBA wild-type (wt) mice (from Charles River Laboratories, Les Oncins, France), *He* knockout mice ($He^{-/-}$) (Cai et al., 2009), pCAGs-eGFP [enhanced green fluorescent protein under the control of a chicken beta-actin promoter and cytomegalovirus enhancer] (Okabe et al., 1997), D1R-eGFP [enhanced green fluorescent protein under the control of D1R] and D2R-eGFP [enhanced green fluorescent protein under the control of D2R] generated by GENSAT (Bertran-Gonzalez et al., 2008; Gong et al., 2003) were used. These strains were maintained by backcrossing to C57BL/6 mice. $He^{-/-}$ mice show high perinatal death as it is described elsewhere (Cai et al., 2009). Genotypes were determined by PCR as described elsewhere (Cai et al., 2009). The day of pregnancy, determined by the first detection of a vaginal sperm plug in daily inspection, was considered embryonic day (E)0.5.

Birth dating, proliferation and tracking experiments *in vivo*

To study neurogenesis in wt and $He^{-/-}$ mice, birth dating experiments were performed as described elsewhere (Martín-Ibáñez et al., 2010). Briefly, pregnant mice were injected intra-peritoneally with bromo deoxyuridine (BrdU; 50 mg/kg; Sigma Chemical Co., St. Louis, MO). BrdU was administered at E12.5, E14.5, and E16.5, and the embryos were subsequently allowed to develop until E18.5, at which point the dams were terminally anesthetized and the embryos were removed and processed for BrdU immunohistochemistry. For a representative scheme, see Fig.1B.

To analyze proliferation in the GZ *in vivo*, E14.5 pregnant mice received a single dose of ethynyl deoxyuridine (EdU; 50 mg/Kg; C10420, Click-iT® EdU Alexa Fluor® 488 Flow Cytometry Assay Kit; Life Technologies S.A., Alcobendas, Madrid). Thirty minutes later they were terminally anesthetized, and the embryos were processed for EdU detection (according to the manufacturer's instructions). The proliferation analysis of other stages such E16.5, P3 and P7 was performed by Ki67 immunohistochemistry as explained below. Although we also performed Ki67 staining at E14.5, it was not reliably detectable at this stage. For this reason we showed the co-labeling between Ki67 and *He* at E16.5.

To study the generation of *He* positive cells, injections of EdU at E13.5 or E14.5, and BrdU at E16.5 into wt pregnant mice were performed and the embryos were allowed to develop until E18.5, at which point the dams were terminally anesthetized and the embryos were removed and processed for *He* and BrdU immunohistochemistry or EdU detection (Life Technologies S.A.). For a representative scheme, see Fig.S4A.

In order to track the origin of dead cells in the MZ, a pulse of EdU was performed at E18.5 in pregnant mice, and the pups were allowed to develop until P3, at which point the brains were recovered and immunohistochemistry was performed against Cleaved caspase 3 (Cell Signaling Technology, Inc. Danvers MA), Nestin GFAP, or NeuN and EdU. For a representative scheme, see Fig.5G.

To study if the lack of Helios could alter the cells entering or exiting the S-phase of the cell cycle, we performed *in vivo* experiments with $He^{-/-}$ and wt mice as previously described (Lange et al., 2009). Briefly, an initial injection of BrdU (50 mg/kg) was performed in $He^{-/-}$ pregnant females at E14.5. After 45 minutes, a second injection of EdU (50 mg/Kg) was performed. Finally, 45 minutes later, the female was sacrificed and the E14.5 embryos were collected and processed to perform immunohistochemistry.

Double staining for BrdU and EdU permitted the identification of two different cell populations: first population - double labeled cells for EdU and BrdU with a punctate staining corresponding to cells entering S phase; second population - cells single labeled for BrdU, corresponding to cells leaving S phase. For a representative scheme, see Fig.4E.

Production of viral particles and cell transduction

To over-express *He*, NSCs were transduced with the pLV-*He*-IRES-eGFP plasmid or the pLV-IRES-eGFP plasmid which encode human *He* and enhanced green fluorescent protein (eGFP) or eGFP alone, respectively. The pLV-IRES-eGFP plasmid was generated as described elsewhere (Urbán et al., 2010). Briefly, MCS-IRES-eGFP was cloned from the pRV-IRES-eGFP plasmid (Genetrix SL, Tres Cantos, Madrid, Spain) using the *Bam*HI and the *Sal*I restriction sites into the pRRLsinPPT plasmid (pRRL) constructed by the Miami Project to Cure Paralysis Viral Vector Core Lab based on the lentiviral transducing plasmid developed by Naldini et al. (Naldini et al., 1996). To construct the pLV-*He*-IRES-EGFP, the human *He* gene from the SPORT6-*He* plasmid (Life Technologies S.A.) was cloned into the *Bam*HI and *Xho*I sites of pLV-IRES-eGFP.

For lentivirus production 293T cells were plated at a density of approximately 6 x 10^4 cells per cm^2. The following day, cells were transfected with a three-plasmid system (the pLV-IRES-eGFP or pLV-*He*-IRES-eGFP plasmids, the plasmid that expresses HIV-1 *gag* and *pol* genes, and the plasmid that expresses vesicular stomatitis virus G) using the calcium phosphate/DNA co- precipitation method. Cells were transfected for 7h and subsequently the medium was removed and replaced with fresh medium. The supernatant from vector-producing 293T cells was collected every 22 h over 3 days. The supernatant was then passed through a 0.45-µm-pore-size filter to remove producer cells

and subjected to 2 centrifugations at 4°C and 25000 x *g* for 120 min to concentrate the virus. The virus-containing pellet was dissolved in 1% BSA. To determine the viral titer, a total of 2 x 10^5 293T cells were inoculated with serial dilutions of concentrated lentivirus. Forty-eight hours after infection, eGFP titers (international units per ml) were determined using a fluorescence-activated cell scanner (FACS).

Neurosphere assay

LGEs from E14.5 wt or *He*$^{-/-}$ mice were dissected out and mechanically disaggregated as described previously (Martín-Ibáñez et al., 2010). Briefly, LGE-derived neurosphere cultures were obtained by seeding 50000 cells/cm^2 in basal medium [Dulbecco's Modified Eagle's Medium (DMEM; Sigma Chemical Co.):F12 (Life Technologies S.A.) (1:1), 0.3% glucose (Sigma Chemical Co.), 0.3 mg/ml glutamine (Life Technologies S.A.), 5 mM HEPES (Life Technologies S.A.), 100 U/ml penicillin, 100 mg/ml streptomycin (Life Technologies S.A.), 4 µg/ml heparin (Sigma Chemical Co.), 4 mg/ml BSA (Sigma Chemical Co.), 1X N2 supplement (Life Technologies S.A.)], supplemented with 20 ng/ml fibroblast growth factor (FGF; Sigma Chemical Co.) and 10 ng/ml epidermal growth factor (EGF; Life Technologies S.A.). Every 5 days neurospheres were collected, dissociated by pipetting approximately 40 times with a P100 micropipette, and plated down in fresh media at a density of 10000 cells/cm^2. All experiments were performed with at least 3-4 independent neurosphere cultures between passages 4-7.

For differentiation studies, the day after plating cells were collected and allowed to attach to coverslips pre-coated with Matrigel^{TM} (Growth Factor Reduced Matrigel Matrix; BD Biosciences, San Agustín de Guadalix, Madrid) in MD1 medium containing: basal medium supplemented with 20 ng/ml FGF (Sigma Chemical Co.). NSCs were differentiated in this medium for three days and then the culture medium

was changed to MD2 containing basal medium supplemented with 2% fetal bovine serum (FBS; Life Technologies S.A.) for 3 additional days. Cells were fixed with 4% paraformaldehyde (PFA; Merck Biosciences Ltd., Nottingham, UK) solution in phosphate-buffered saline, pH 7.4 (PBS) and processed for immunocytochemistry analyses. Loss of function (LOF) experiments were performed with neurospheres derived from *He*$^{-/-}$ mice and compared to the control neurospheres derived from wt mice. Gain of function (GOF) experiments were performed by over-expressing *He* via the transduction of neurospheres the first day after plating with pLV-*He*-IRES-eGFP lentivirus or the control pLV-IRES-eGFP. The number of neurons (positive for β-III-tubulin) and astrocytes (positive for GFAP) were analyzed after 6 days in differentiation in LOF and GOF experiments. Results are expressed as the percentage of cells positive for each marker. All experiments were performed with at least 3-4 independent neurosphere cultures between passages 4-7.

Cell Cycle analysis *in vitro*

Proliferation assays

BrdU incorporation assays were performed in wt and *He*$^{-/-}$ mice derived neurospheres (for LOF experiments) and neurospheres over-expressing pLV-*He*-IRES-eGFP or pLV-IRES-eGFP (for GOF experiments) as described elsewhere (Urbán et al., 2010). LOF experiments were performed by seeding 25000 cells in a P24 well plate in proliferative conditions and after three days the cells were treated with 1μM BrdU (Sigma Chemical Co.) for 20 minutes, collected and incubated for 10 minutes in P24 well plates containing glass coverslips pre-coated with Matrigel^{TM} (BD Biosciences) to enhance attachment of cells to the surface. Immediately after incubation, cells were fixed with 4% PFA solution. Once fixed, neurosphere preparations were incubated for 30 min in 2N HCl followed by treatment with Sodium Borate 0.1M for 20 minutes and processed

for immunocytochemistry against BrdU. For GOF experiments, 25000 cells were seeded in a P24 well plate in proliferative conditions and infected with pLV-*He*-IRES-eGFP or the control pLV-IRES-eGFP lentivirus using a multiplicity of infection (MOI) of 2.5. After cell transduction, the BrdU assay was performed following the protocol described for wt and $He^{-/-}$ neurospheres. The percentage of cells incorporating BrdU was quantified.

The same cultures were processed for immunocytochemistry against Ki67 to further analyze the percentage of proliferating cells in LOF and GOF experiments. These experiments were performed with at least 3-4 independent neurosphere cultures between passages 4-7.

Cell cycle length

An accumulative exposure to 1µM BrdU during 36 hours was performed in wt and $He^{-/-}$ mice derived neurospheres (LOF) and in neurospheres over-expressing pLV-*He*-IRES-eGFP or pLV-IRES-eGFP (GOF) after 2DIV in proliferation. At different time points after 1µM BrdU exposure (1, 3, 6, 12, 24 and 36 hours), cells were collected and incubated for 10 minutes in P24 well plates containing glass coverslips pre-coated with Matrigel™ (BD Biosciences) to enhance attachment of cells to the surface. Immediately after incubation cells were fixed with 4% PFA solution and processed for BrdU immunocytochemistry. Analysis of the percentage of BrdU positive cells over time gives rise to a curve that at a certain time point reaches a plateau phase, where all the cells in proliferation are labeled with BrdU. Following a regression analysis as previously described by Takahashi et al (Takahashi et al., 1992; Takahashi et al., 1995), the length of the cell cycle and the length of the S phase were calculated for the NPCs in the presence and absence of *He*. These experiments were performed with at least 3-4 independent neurosphere cultures between passages 4-7.

S-phase analysis

To study the cells entering and exiting the S-phase of the cell cycle, we performed *in vitro* experiments with neurospheres derived from *He*$^{-/-}$ and wt mice as previously described (Lange et al., 2009). Briefly, an initial pulse of 1µM BrdU was performed in a culture of proliferating neurospheres growing for 2 days in vitro (2DIV). Then, after 45 minutes a second pulse of 1µM EdU was performed. After a further 45 minutes cells were collected and incubated for 10 minutes in P24 well plates containing glass coverslips pre-coated with Matrigel™ (BD Biosciences) to enhance attachment of cells to the surface. Immediately after incubation cells were fixed with 4% PFA solution and processed for immunocytochemistry. The percentage of double for EdU and BrdU with a punctate staining corresponding to cells entering S phase or single labeled cells for BrdU corresponding to cells leaving S phase were quantified for wt and *He*$^{-/-}$ mice derived neurospheres (see representative scheme in Fig.4E). These experiments were performed with at least 3-4 independent neurosphere cultures between passages 4-7.

G_2/M phase labeling

To study the combined length of the G_2/M phases, an accumulative exposure to 1µM BrdU over 5 hours was performed in wt and *He*$^{-/-}$ mice derived neurospheres (LOF) and neurospheres over-expressing pLV-*He*-IRES-eGFP or pLV-IRES-eGFP (GOF) after 2 DIV in proliferation. At different time points (30 minutes, 1, 2, 3, 4 and 5 hours), cells were collected and incubated for 10 minutes in P24 well plates containing glass coverslips pre-coated with Matrigel™ (BD Biosciences) to enhance attachment of cells to the surface. Immediately after incubation cells were fixed with 4% PFA solution and processed for BrdU immunocytochemistry. Analysis of the mitotic BrdU labeling index was performed as described previously (Takahashi et al., 1995). The percentage of mitotic cells positive for BrdU was counted at each time point for both cell cultures.

The time required to label all mitotic figures with BrdU is considered as the length of the combined G_2/M phases (Takahashi et al., 1995). These experiments were performed with at least 3-4 independent neurosphere cultures between passages 4-7.

Cell cycle index

We analyzed cell cycle index as the number of cells that retain BrdU but leave the cell cycle (abandoned the G_1-S-G_2/M phases and entered into G_0) as previously described (Urbán et al., 2010). These experiments were performed in wt and *He*$^{-/-}$ mice derived neurospheres (for LOF experiments) and neurospheres over-expressing pLV-*He*-IRES-eGFP or pLV-IRES-eGFP (for GOF experiments). Briefly, 25000 cells were seeded in a P24 well plate in proliferative conditions and after two days the cells were treated for 24 hours with 1µM BrdU (Sigma Chemical Co.), collected and incubated for 10 minutes in P24 well plates containing glass coverslips pre-coated with Matrigel™ (BD Biosciences) to enhance attachment of cells to the surface. Immediately after incubation, cells were fixed with 4% PFA solution. Double immunohistochemistry against BrdU and Ki67 was performed, and the combination of these markers allowed the quantification of the fraction of cell cycle index (cells that abandoned cell cycle and entered into G_0, single labeled with BrdU) or cells still in proliferation (double labeled with BrdU and Ki67). For a representative scheme see Fig.S13A. These experiments were performed with at least 3-4 independent neurosphere cultures between passages 4-7.

Discerning high and low Ki expressing cells

We detected high and low expressing KI67 cells with the automatic intensity detection of the Cell Profiler software. Briefly the grayscale 16 bit images from each color channel were included in an automated pipeline that identified objects within the range of typical diameter of 15 to 45 pixels (IdentifyPrimaryObjects module), then its shape

and intensity was measured (MeasureObjectIntensity module), we visualized the results in an histogram of intensities distribution where two populations were easily separated. We determined the appropriate threshold (0.03 AU) to distinguish between high and low intensity objects.

Analysis of the He binding sites at the *Ccne* promoter

In order to corroborate the binding of Helios with promoter regions detected on the Cyclin E gene (Ccne1) we obtained the Big Wig file from the GEO repository of the article by (Kim et al., 2015) (GEO Series GSE72997), and visualized it in the Integrative Genome Viewer with the files provided aligned to the Ensembl Mouse Genome [version mm9; http://www.ensembl.org/Mus_musculus/Info/Index; European Bioinformatics Institute (EMBI-EBI) and the Wellcome Trust Sanger Institute (WTSI); Wellcome Trust Genome Campus; Hinxton, UK].

Western blots

We analyzed cell cycle protein levels in LOF and GOF *in vitro* and *in vivo*: neurospheres overexpressing *He* or eGFP, $He^{-/-}$ and wt neurospheres, and $He^{-/-}$ or wt E14.5 LGEs. Samples were prepared and processed for western blot as described elsewhere (Canals et al., 2004). Briefly, samples were homogenated by BioRuptor Sonicator (Diagenode) in 100 µl assay buffer (50 mM Tris-HCl, pH 7.5; 150 mM NaCl; 10% glycerol; 10 mM EGTA, 1% Triton X-100; 100mM NaF; 5µM $ZnCl_2$; 1 µg/ml Leupeptin; 8 µl/ml PMSF; 1 µg/ml Aprotinin and 2.5 µl/ml Orthovanadate). Between fifteen and twenty micrograms of the homogenates were loaded in a 10% SDS-PAGE (sodium dodecyl sulfate-polyacrylamide gel electrophoresis) and transferred to Immobilon-P membranes (Milipore, Bedford, MA). Blots were incubated overnight at 4°C with 1:750 of anti-CyclinE antibody (M-20, rabbit polyclonal; Santa Cruz

Biotechnology Inc), 1:750 of anti-E2F1 antibody (Sc-251, Santa Cruz Biotechnology Inc), 1:750 of anti-retinoblastoma (Rb) antibody (C15, Santa Cruz Biotechnology Inc) or anti-PCNA (PC-10, Santa Cruz Biotechnology Inc.), and after several washes in Tris-buffered saline containing 0.1% v/v Tween-20 (TBS-T), membranes were incubated with an HRP-conjugated anti-rabbit IgG (1:1000; Promega) or anti-mouse IgG (1:1000; Promega) and developed with the western blotting luminol reagent ImmunoCruz (sc-2048, Santa Cruz Biotechnology, Inc.). Western blots were quantified using the Gel-Pro analyzer.

In situ hybridization

To asses which striatal subpopulation of MSNs express *He*, we performed double *in situ* hybridization for enkephalin (ENK) or tackikinin A [(Tac1, a precursor of Substance P(SP)] and immunohistochemistry for *He* as described previously (Martín-Ibáñez et al., 2010). Frozen tissue sections were air dried, fixed in 4% paraformaldehyde in PBS for 20 min at 4°C and washed in 0.1% Diethyl pyrocarbonate (DEPC; Sigma Aldrich)-PBS for 5 min. Slides were carbethoxylated in 0.1% DEPC-PBS for 10 min at r.t. Slides were washed once in 0.1% DEPC-PBS at r.t. for 1 min and twice in 0.2% DEPC-Sodium Salt Citrate (1× SSC: 150 mM NaCl, 15 mM sodium citrate) at r.t. for 2 min. Thereafter, sections were incubated with prehybridization buffer (50% formamide, 5× SSC, 5× Denhardt's solution, 250 µg/ml yeast tRNA and 500 µg/ml salmon sperm DNA) at 56ºC for 3h in a humidified chamber, and finally hybridized overnight at 56ºC with 300 µl of the same prehybridization buffer containing the oligodeoxyribonucleotide probes previously labeled with terminal deoxynucleotidyltransferase and digoxigenin (DIG)-11-dUTP (Roche). The day after, slides were washed at 56ºC with 5× DEPC-SSC 2 min, 5× DEPC-SSC 5 min, 2x DEPC-SSC 5 min, 0.2× DEPC-SSC 5 min, 50 % Formamide in 0.2× DEPC-SSC for 20 min,

0.2× DEPC-SSC 5 min and 1x Tris buffered saline containing with 1 % v/v of tween-20 (TBS-T) for 5 min at room temperature . To develop the signal, slides were blocked with 3% milk in TBS-T for 1h, and were incubated with the anti DIG-AP-Antibody (1:5000, Roche) in blocking buffer for 1h at r.t. Finally, in situ was developed by incubating the sections with 3.3 mg nitroblue tetrazolium and 1.65 mg bromochloroindolyl phosphate (Invitrogen S.A.) dissolved in 10 ml alkaline buffer (10X Stock: 60.5g Tris-base + 29.2g NaCl in mQ Water, pH 9.5). The enzymatic reaction was stopped by extensive rinsing in alkaline buffer with the addition of 1 mM EDTA. Next day, slides were washed with 1x Tris-EDTA buffer (TE, 10X Stock: 12.1g Tris-Base + 3.72g EDTA) and they were processed for immunohistochemistry as described previously.

Immunolabeling

Immunostainings were performed using the following antibodies: anti-*He* [1:5000 for cells and 1:1000 for tissue; polyclonal; a generous gift of Dr. Stephen T. Smale (Howard Hughes Medical Institute, Molecular Biology Institute, and Department of Microbiology and Immunology, UCLA School of Medicine, Los Angeles, CA, USA), (Hahm et al., 1998)], anti-*He* (1:50; polyclonal; Santa Cruz Biotechnology Inc.) anti-nestin (Rat 401; 1:50; polyclonal; Developmental Studies Hybridoma Bank; The University of Iowa, Iowa), anti-GFAP (1:200; monoclonal; Sigma Chemical Co.), anti-β-III-tubulin (Tuj1; 1:200; Sigma Chemical Co.), anti-MAP2 (1:500; monoclonal; Sigma Chemical Co.), anti-MAP2 (1:500; polyclonal; Abcam, Cambridge, UK), anti-NeuN (1:100; monoclonal; Merck KGaA, Darmstadt, Germany), anti- dopamine- and cAMP-regulated phosphoprotein of 32 kDa (DARPP-32; 1:500; polyclonal; BD Biosciences), anti-enkephalin (1:2000; polyclonal; ImmunoStar, Inc., Hudson, WI, USA), anti-calbindin (1:1000; monoclonal; Sigma Chemical Co.), anti-parvalbumin

(1:1000; polyclonal; SWANT, Bellinzona, Switzerland), anti-Choline Acetyl Transferase (ChAT; 1:500; polyclonal; Life Technologies S.A.), anti-Cleaved Caspase-3 (1:200; polyclonal; Cell Signaling Technology), anti-*Ctip2* (1:400; polyclonal: Abcam), anti-Ki67 (NCL-L-ki67-MM1; 1:100; monoclonal; Leica Microsistemas S.L.U. Barcelona), anti-Ki67 (1:50; monoclonal [SP6]; Abcam); anti-Phospho-Histone H3 (PH3; 1:200; Monoclonal; Cell Signaling Technology), anti-BrdU (1:50; monoclonal; Dako A/S, Glostrup, Denmark), GFP-FITC (1:200; polyclonal; Abcam), TUNEL (DeadEnd™ Fluorometric TUNEL System; Promega Biotech Ibérica SL, Alcobendas, Madrid) and EdU (C10420, Click-iT® EdU Alexa Fluor® 488 Flow Cytometry Assay Kit; Life Technologies S.A.).

All these antibodies were previously used and validated in (Bosch et al., 2004; Canals et al., 2004; Martín-Ibáñez et al., 2010; Pineda et al., 2005).

For histological preparations embryonic or postnatal brains were removed at specific developmental stages and were frozen in dry-ice cooled methyl-butane (Sigma Chemical Co.). Serial coronal cryostat sections (14 μm) were cut on a cryostat and collected on silane-coated slides and frozen at -20^{o}C.

Fluorescent immunolabeling was performed according to the protocol described in (Bosch et al., 2004). Briefly, cultures were fixed with 4% PFA for 20 min. Cultures and/or tissue sections were blocked for 1 h in PBS containing 0.3% Triton X-100 and 1% bovine serum albumin (BSA) to avoid non specific binding. For BrdU labeling an initial permeabilization treatment was performed before the blocking step. This was achieved by incubating cultures or tissue sections for 30 minutes or 90 minutes, respectively, in 2N HCl followed by a 20 minute wash in sodium borate 0.1M. Following the blocking step samples were incubated overnight at 4°C in PBS containing 0.3% Triton X-100 and 1% BSA with the corresponding primary antibodies. After three

PBS washes, cultures or tissue sections were incubated for 2 h at room temperature (r.t.) with the following secondary antibodies: Cy3-conjugated donkey anti-rabbit IgG (1:500) or Cy2-conjugated donkey anti-mouse (1:200; all from Jackson Immunoresearch Laboratories Inc., West Grove, PE, USA). Cultures or tissue sections were counterstained with 4,6'-diamidino-2-phenylindole (DAPI; Sigma Chemical Co.) and mounted in Mowiol (Calbiochem, La Jolla, CA, USA). No signal was detected in control preparations from which the primary antibody was omitted. Fluorescent photomicrographs were taken on a Leica TCS SL laser scanning confocal spectral microscope (Leica Microsistemas S.L.U.). All images were acquired as tiff files and adjustments of brightness and contrast were performed with Adobe Photoshop 6.0 (Adobe Systems Incorporated).

To analyze the cellular populations of the adult striatum, 5-6 weeks old wt and *He*$^{-/-}$ mice were transcardially perfused with 4% PFA. Brains were removed, postfixed for 2 hours at 4°C in the same solution, cryoprotected in PBS containing 30% sucrose, and frozen in dry ice-cooled methyl-butane (Sigma Chemical Co.). Serial coronal cryostat sections (30 µm thick) through the whole striatum were collected as free-floating sections in PBS and processed for diaminobenzidine immunohistochemistry as described previously (Canals et al., 2004). Briefly, endogenous peroxidases were blocked for 30–45 min in PBS containing 3% H_2O_2. Subsequently, nonspecific protein interactions were blocked with normal serum or bovine serum albumin. Samples were incubated overnight at 4ºC with the corresponding primary antibodies. Sections were washed three times in PBS and incubated with a biotinylated secondary antibody (1:200; Thermo Fisher Scientific Inc., Rockford, IL, USA) at r.t. for 2 h. The immunohistochemical reaction was developed using the ABC kit (Thermo Fisher Scientific Inc.) and visualized with diaminobenzidine. No signal was detected in control

preparations from which the primary antibody was omitted. Cresyl violet staining was performed as described previously (Giralt et al., 2010).

Measurement of volumes and *in vivo* cell counts

The volumes of certain brain regions were measured using ImageJ v1.33 on a computer attached to an Olympus microscope (Olympus Danmark A/S, Ballerup, Denmark). Consecutive 30 µm-thick sections (14–16 sections/animal) for adult mice and 14-µm-thick sections for embryos were viewed, and the borders of the anatomical landmarks were outlined. The volumes were calculated by multiplying the sum of all section areas (mm^2) by the distance between successive sections (0.3 mm) as described previously (Canals et al., 2004). All cell counts (EdU and Ki67 for GZ proliferation; BrdU for birth dating experiments; Cleaved Caspase 3 for cell death; Ctip2, Calbindin, DARPP-32, ChAT and Parvalbumin for striatal cell population) were genotype-blind (n: 4–6 per each condition). Nuclear stained cells were counted for BrdU, Ki67, EdU, Ctip2 and Cleaved Caspase 3. For the rest of the markers those cells showing a clear positive cytoplasm surrounding a less well-stained nucleus were counted. Unbiased stereological counts were performed using the Computer Assisted Stereology Toolbox (CAST) software (Olympus Danmark A/S). Stereological cell counts cover all striatal area for each animal. Dorso-medial (DM), dorso-lateral (DL), ventro-medial (VM) and ventro-lateral (VL) striatal areas were specifically counted along the rostrocaudal axis for DARPP-32, ENK and SP positive cells. These cell counts were also done by unbiased stereological counts using the CAST software.

The number of positive cells in the striatum, GZ or MZ was estimated using the optical dissector method (Gundersen et al., 1988). A grid size was chosen so that 10% of total striatal, GZ or MZ area was counted. The unbiased counting frame was positioned randomly on the outline of the striatum, GZ, or MZ by the software, thereby

creating a systematic random sample of the area. Sections were viewed under a 100x objective, and the counting field corresponded to 1,529.00 μm^2. Gundersen coefficients of error were all less than 0.10. For striatal cell counts, sections spaced 240 μm apart were analyzed. For GZ and MZ cell counts, sections spaced 140 μm apart were analyzed.

The distribution of mitosis in *He*$^{-/-}$ and wt striatum at E16.5 was analyzed as described in (Pilz et al., 2013). Briefly, E16.5 slides were stained for PH3 as described previously, and mitotic cells of the striatal GZ were classified into three types of progenitors: PH3+ cells in the border of the ventricle generated Apical progenitors (AP); PH3+ cells inside the VZ conformed Subapical progenitors (SAP) and Basal progenitors (BP) were PH3+ cells in the SVZ. PH3+ cells were counted using CAST software.

Quantification of double positive cells for *He* and D2R, D1R, ENK or SP were done by counting the number of double positive cells on five coronal sections per animal spaced 100 μm apart (*n*=3 animals per condition). Results are expressed as the percentage of *He* + cells that express D2R, D1R, ENK or SP, considering the total *He* + cells as the 100%.

Quantification of Cleaved caspase 3 + cells that were double positive for Nestin, GFAP or NeuN were done by counting the number of double positive cells on five coronal sections per animal spaced 100 μm apart (*n*=3 animals per condition). Total number of Cleaved caspase 3+ cells were considered 100%.

Automated quantification of branches, and neurite length was performed using Cell Profiler v2.8 software (pipeline available upon request), briefly, cell somas were manually selected and a secondary object recognition of morphology was performed using somas as seeds, the modules Morph/skeletonize and MeasureNeurons were then

used to obtain each neuron branching graph with measurements of every neurite. (GFP n=47, He=22). All the analysis was performed in a blinded fashion.

Q-PCR

Gene expression was evaluated by Q-PCR assays as previously described by Martin-Ibanez et al. (Martín-Ibáñez et al., 2010). The following TaqMan® and IDT Gene expression Assays (Applied Biosystems, Foster City, CA and Integrated DNA Technologies, BVBA, Belgium, respectively) were used: 18s, Hs99999901_s1; *Gsx2*, Mm00446650_m1; *Ascl1*, Mm03058063_m1; *Dlx1*, Mm00438424_m1; *Dlx2*, Mm00438427_m1; *Dlx5*, Mm00438430_m1; *Dlx6*, Mm01166201_m1; *Ebf1*, Mm00395519_m1; *Eos*, Mm00617657_m1; *Peg*, Mm00731061_s1; *He*, Mm00496108_m1.; *Ccne*, Mm.PT.58.8618916. To provide negative controls and exclude contamination by genomic DNA, the reverse transcriptase was omitted in the cDNA synthesis step, and the samples were subjected to the PCR reaction with each TaqMan® gene expression assay.

Analysis and quantification was performed with the Comparative Quantitation Analysis program of the MxPro™ Q-PCR analysis software version 3.0 (Stratagene, La Jolla, CA, USA), using the 18S gene expression as internal loading control. All Q-PCR assays were performed in duplicate and repeated for at least three independent experiments. The results were expressed as relative levels with respect to the expression of the same gene in E14.5 for developmental studies or the control vector over-expressing cells considered as 100%.

Primary striatal culture and transfection

E14.5 fetal brains from wt embryos were excised and the LGEs were dissected and cultured as previously described (Martín-Ibáñez et al., 2010). For *He* over-expression

studies, cells were transfected with the MSCV-*He*-IRES-eGFP plasmid, or with the MSCV-IRES-eGFP plasmid as a control (Zhang et al., 2007). Primary cultures were transfected 24 hours after seeding with 0.5 µg of the corresponding plasmids per well (24-well plate). The transfection was performed using Lipofectamine LTX (Life Technologies S.A.), accordingly to the manufacturer instructions, which results in a transfection efficiency of 0.5-1% of the cells. Three days after transfection cells were fixed with 4% PFA for immunocytochemistry analysis. We counted the number of *He* or eGFP overexpressing cells per coverslip that co-localized with different markers, such as calbindin, DARPP-32 and enkephalin. The results were expressed as the percentage of transfected cells co-localizing with the different markers with respect to the total number of transfected cells. These experiments were performed with at least 3-4 independent LGE primary cultures.

Cell transplants

Prior to transplantation, eGFP mice derived neurospheres were transduced with either *He* or eGFP were harvested and resuspended in PBS. P2-P3 neonatal mice were anesthetized by hypothermia, placing them on ice until cessation of movement. Unilateral striatal injections were performed using a stereotaxic apparatus (Davis Kopf Instruments, Tujunga, CA, USA) and a 10 µl Hamilton syringe with a 33 gauge needle (Hamilton, Reno, NV), setting the following coordinates (millimeters): AP, +2.3, L, +1.4 from lambda and DV, -1.8 from dura. Every animal received 10000 cells diluted in 1 µl of PBS. Upon completion of stereotaxic surgery, pups were warmed, monitored for 1h to ensure recovery and then returned to the housing facility for 2 or 4 weeks.

Quantification of transplanted cells was performed by counting the number of GFP^{+}/DARPP-32 + neurons on five coronal sections per animal spaced 100 µm apart

(*n*=3 animals per condition). All GFP positive cells were examined for DARPP-32 + immunostaining.

Mouse Behavior

Swimming task

The apparatus consisted of a transparent perspex extended swimming tank (100 cm long, 10 cm wide with walls measuring 40 cm high). Water level was 20 cm from floor to surface, and it was maintained at 26°C ± 1. A black screen surrounded the tank to avoid the vision of distal cues. Testing conditions were carried out in dimly light conditions (100 lux). The mice were placed in an extreme of the swimming tank facing away from a visible escape platform (10 cm wide, 10 cm long and with a 10 cm high with the top surface 0.5 cm above the water level) at one end of the tank. The time required to reach the platform (escape latencies) in these trials was recorded. Two blocks of three trials with an inter-block interval of 24 h were performed.

Balance beam

A beam consisted of a long steel cylinder (50 cm) with a 50 mm-square cross-section and a 15 mm-round diameter. The beam was placed horizontally, 50 cm above the bench surface, with each end mounted on a narrow support. Animals were allowed to walk along the beam until they reach 30 cross-sections (5 cm each), while their latency to fall and number of falls were measured.

Rotarod

Acquisition of a motor coordination task was further evaluated on the rotarod apparatus at fixed rotations per minute (rpm). In brief, animals at 5 weeks of age were trained at constant speed (24 rpm) for 60 sec. We performed three trials per day for two

consecutive days; and the latency to fall and the number of falls during 60 sec was recorded.

Footprint test

Mice were trained to walk in a corridor that was 50 cm long and 7 cm wide. The forefeet and hindfeet of the mice were painted with non-toxic red and blue ink, respectively, and then given one run. The footprint pattern was analyzed for the general pattern and stride length was measured as the average distance of forward movement between each stride, and the forebase and hindbase widths were measured as the perpendicular distance between the left and right footprints of a given step.

References

Bertran-Gonzalez, J., Bosch, C., Maroteaux, M., Matamales, M., Hervé, D., Valjent, E. and Girault, J.-A. (2008). Opposing patterns of signaling activation in dopamine D1 and D2 receptor-expressing striatal neurons in response to cocaine and haloperidol. *J. Neurosci.* **28**, 5671–85.

Bosch, M., Pineda, J. R., Suñol, C., Petriz, J., Cattaneo, E., Alberch, J. and Canals, J. M. (2004). Induction of GABAergic phenotype in a neural stem cell line for transplantation in an excitotoxic model of Huntington's disease. *Exp. Neurol.* **190**, 42–58.

Cai, Q., Dierich, A., Oulad-Abdelghani, M., Chan, S. and Kastner, P. (2009). Helios deficiency has minimal impact on T cell development and function. *J. Immunol.* **183**, 2303–11.

Canals, J. M., Pineda, J. R., Torres-Peraza, J. F., Bosch, M., Martín-Ibañez, R., Muñoz, M. T., Mengod, G., Ernfors, P. and Alberch, J. (2004). Brain-derived neurotrophic factor regulates the onset and severity of motor dysfunction associated with enkephalinergic neuronal degeneration in Huntington's disease. *J. Neurosci.* **24**, 7727–39.

Giralt, A., Friedman, H. C., Caneda-Ferrón, B., Urbán, N., Moreno, E., Rubio, N., Blanco, J., Peterson, A., Canals, J. M. and Alberch, J. (2010). BDNF regulation under GFAP promoter provides engineered astrocytes as a new approach for long-term protection in Huntington's disease. *Gene Ther.* **17**, 1294–308.

Gong, S., Zheng, C., Doughty, M. L., Losos, K., Didkovsky, N., Schambra, U. B., Nowak, N. J., Joyner, A., Leblanc, G., Hatten, M. E., et al. (2003). A gene expression atlas of the central nervous system based on bacterial artificial chromosomes. *Nature* **425**, 917–925.

Gundersen, H. J., Bagger, P., Bendtsen, T. F., Evans, S. M., Korbo, L., Marcussen, N., Møller, A., Nielsen, K., Nyengaard, J. R. and Pakkenberg, B. (1988). The new stereological tools: disector, fractionator, nucleator and point sampled intercepts and their use in pathological research and diagnosis. *APMIS* **96**, 857–81.

Hahm, K., Cobb, B. S., McCarty, A. S., Brown, K. E., Klug, C. A., Lee, R., Akashi, K., Weissman, I. L., Fisher, A. G. and Smale, S. T. (1998). Helios, a T cell-restricted Ikaros family member that quantitatively associates with Ikaros at centromeric heterochromatin. *Genes Dev.* **12**, 782–96.

Kim, H.-J., Barnitz, R. A., Kreslavsky, T., Brown, F. D., Moffett, H., Lemieux, M. E., Kaygusuz, Y., Meissner, T., Holderried, T. A. W., Chan, S., et al. (2015). Stable inhibitory activity of regulatory T cells requires the transcription factor Helios. *Science (80-.).* **350**, 334–339.

Lange, C., Huttner, W. B. and Calegari, F. (2009). Cdk4/cyclinD1 overexpression in neural stem cells shortens G1, delays neurogenesis, and promotes the generation and expansion of basal progenitors. *Cell Stem*

Cell **5**, 320–31.

Martín-Ibáñez, R., Crespo, E., Urbán, N., Sergent-Tanguy, S., Herranz, C., Jaumot, M., Valiente, M., Long, J. E., Pineda, J. R., Andreu, C., et al. (2010). Ikaros-1 couples cell cycle arrest of late striatal precursors with neurogenesis of enkephalinergic neurons. *J. Comp. Neurol.* **518**, 329–51.

Naldini, L., Blömer, U., Gage, F. H., Trono, D. and Verma, I. M. (1996). Efficient transfer, integration, and sustained long-term expression of the transgene in adult rat brains injected with a lentiviral vector. *Proc. Natl. Acad. Sci. U. S. A.* **93**, 11382–8.

Okabe, M., Ikawa, M., Kominami, K., Nakanishi, T. and Nishimune, Y. (1997). “Green mice” as a source of ubiquitous green cells. *FEBS Lett.* **407**, 313–9.

Pilz, G.-A., Shitamukai, A., Reillo, I., Pacary, E., Schwausch, J., Stahl, R., Ninkovic, J., Snippert, H. J., Clevers, H., Godinho, L., et al. (2013). Amplification of progenitors in the mammalian telencephalon includes a new radial glial cell type. *Nat. Commun.* **4**, 2125.

Pineda, J. R., Canals, J. M., Bosch, M., Adell, A., Mengod, G., Artigas, F., Ernfors, P. and Alberch, J. (2005). Brain-derived neurotrophic factor modulates dopaminergic deficits in a transgenic mouse model of Huntington’s disease. *J. Neurochem.* **93**, 1057–68.

Takahashi, T., Nowakowski, R. S. and Caviness, V. S. (1992). BUdR as an S-phase marker for quantitative studies of cytokinetic behaviour in the murine cerebral ventricular zone. *J. Neurocytol.* **21**, 185–97.

Takahashi, T., Nowakowski, R. S. and Caviness, V. S. (1995). The cell cycle of the pseudostratified ventricular epithelium of the embryonic murine cerebral wall. *J. Neurosci.* **15**, 6046–57.

Urbán, N., Martín-Ibáñez, R., Herranz, C., Esgleas, M., Crespo, E., Pardo, M., Crespo-Enríquez, I., Méndez-Gómez, H. R., Waclaw, R., Chatzi, C., et al. (2010). Nolz1 promotes striatal neurogenesis through the regulation of retinoic acid signaling. *Neural Dev.* **5**, 21.

Zhang, Z., Swindle, C. S., Bates, J. T., Ko, R., Cotta, C. V and Klug, C. A. (2007). Expression of a non-DNA-binding isoform of Helios induces T-cell lymphoma in mice. *Blood* **109**, 2190–7.

SUPPLEMENTARY FIGURES

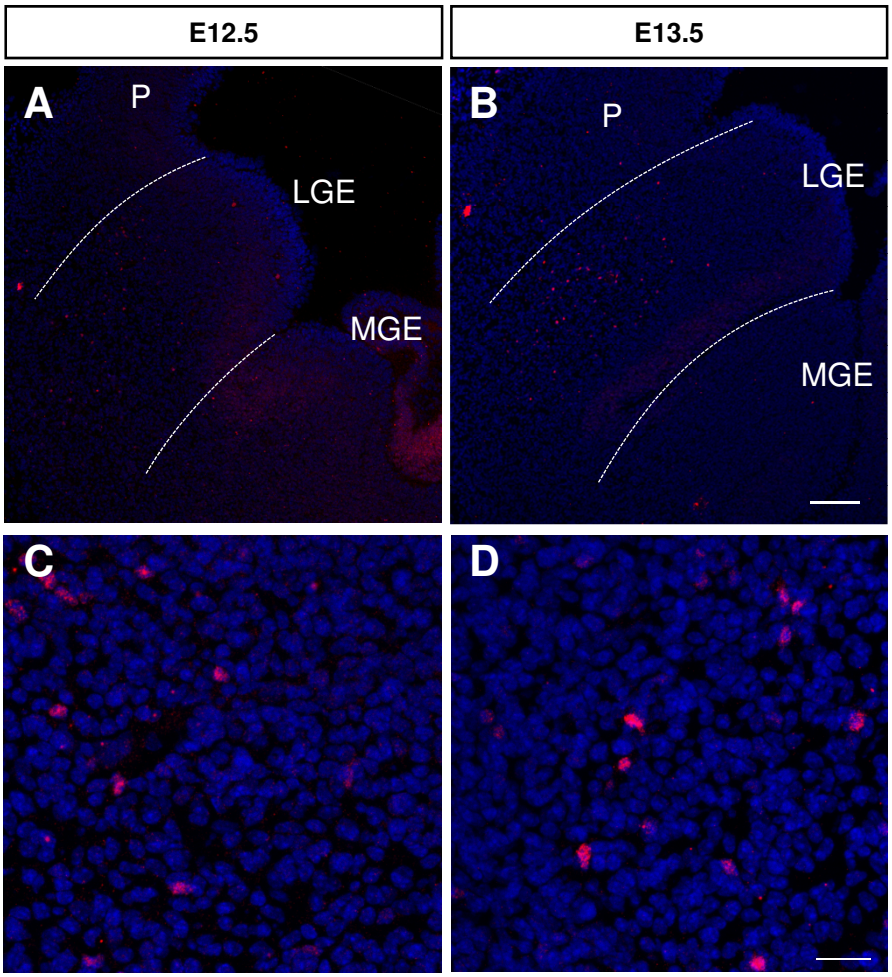

Figure S1. *He* is expressed at early embryonic developmental stages in scattered cells. (**A,C**) Immunohistochemistry for *He* at E12.5 at low (**A**) or high magnification (**C**). (**B,D**) Immunohistochemistry for *He* at E13.5 at low (**B**) or high magnification (**D**). Scale bars; A-B; 100 μm, C-D; 20 μm.

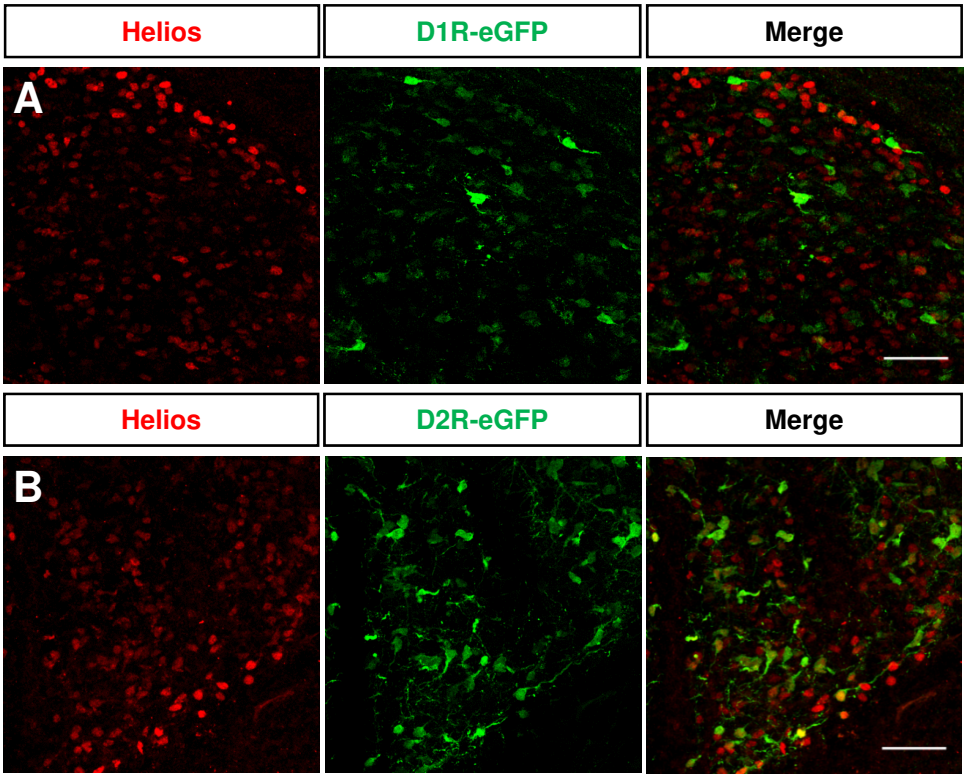

Figure S2. *He* mainly co-localizes with D2R + neurons in the striatum. (**A**) Double immunohistochemistry against *He* and GFP in the D1R-eGFP mice showing few double stained cells. This representative image is taken from de dorsolateral striatum at P3. (**B**) Double immunohistochemistry against *He* and GFP in the D2R-eGFP mice showing a higher percentage of *He* expressing cells co-localizing with D2R positive neurons. This representative image is taken from de ventrolateral striatum at P3. Scale bars: 50μm.

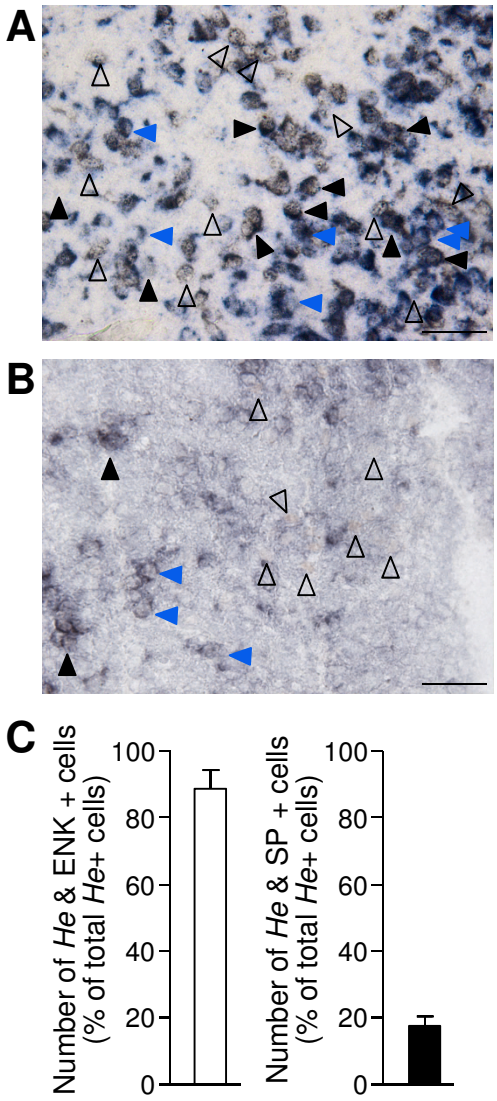

Figure S3. Helios is mainly expressed by ENK + neurons in the striatum. (**A**) Double *in situ* for ENK (dark blue) and *He* immunohistochemistry (brown) show a high percentage of colocalization (black closed arrowheads) but few *He* + cells were not ENKergic neurons (open arrowheads). In addition, some ENK + neurons were negative for *He* (blue closed arrowheads). This representative image is taken from the dorsomedial striatum at P7. (**B**) Double *in situ* for tachykinin A, the precursor of substance P, (dark blue) and *He* immunohistochemistry (brown) show low percentage of colocalization (black closed arrowheads) but many single labeled *He* + cells (open arrowheads). In addition, many tachykinin A + neurons were negative for *He* (blue closed arrowheads). This representative image is taken from the dorsolateral striatum at P7. Scale bars; 50 μm. (**C**) Quantification of the percentage of *He*+ cells that co-express ENK or SP.

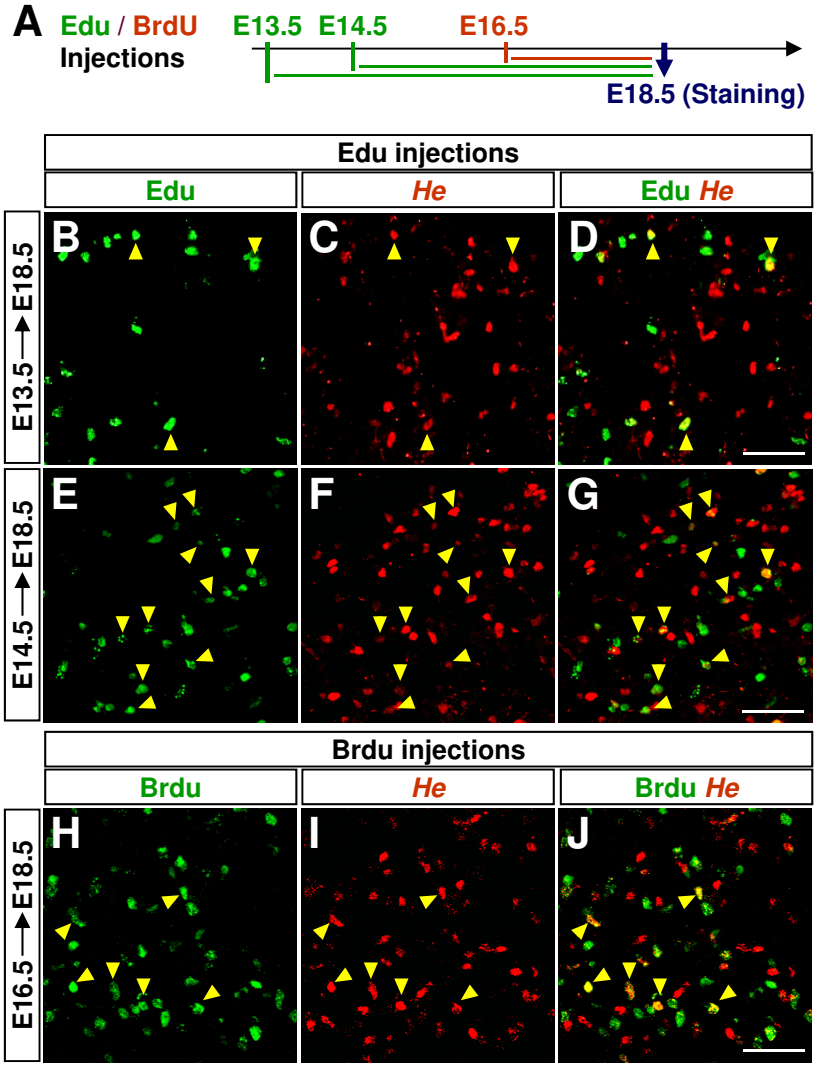

Figure S4. *He* is expressed by cells generated at late striatal neurogenic stages. (**A**) Schematic representation of double EdU and BrdU injections performed at E13.5, E14.5 and E16.5, respectively. To analyze the birth-date of *He* expressing cells, double immunohistochemistry against EdU or BrdU and *He* was performed at E18.5. (**B-D**) Double immunohistochemistry against EdU and *He* demonstrated that few of the *He*-positive cells are generated at E13.5. Yellow arrowheads point to double positive cells in a representative image taken in the mid-striatum. Scale bar: 50 μm. (**E-G**) Double immunohistochemistry against EdU and *He* demonstrated that a higher percentage of *He*-positive cells are generated at E14.5. Yellow arrowheads point to double positive cells in a representative image taken in the mid-striatum. Scale bar: 50 μm. (**H-J**) Double immunohistochemistry against BrdU and *He* demonstrated that some *He*-positive cells are generated at E16.5. Yellow arrowheads point to double positive cells in a representative image taken in the mid-striatum. Scale bar: 50 μm.

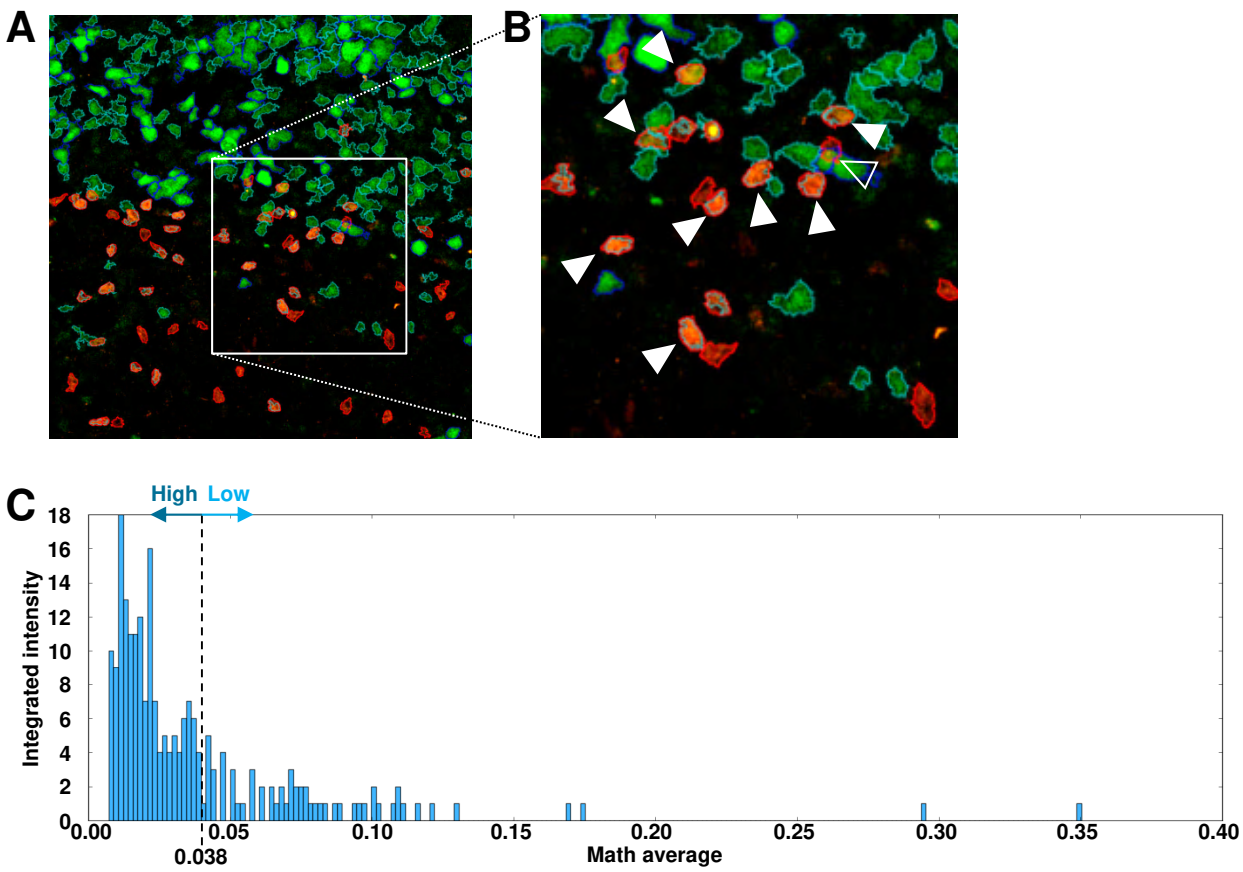

Figure S5. High and low Ki67 expressing cells were analyzed by using the Cell Profiler program. (**A**) Representative picture of the automatic detection of high expressing Ki67 cells (dark blue), low expressing Ki67 cells (light blue) and He expressing cells (red). (**B**) As evidenced in the image only 1 cell with high expression of Ki67 partially overlaps with He expression (open arrowhead), whereas the rest of Ki67/He+ve cells are low expressing (close arrowhead). (**C**) Graft representing the intensity of Ki67 expressing cells and cut off at 0.038.

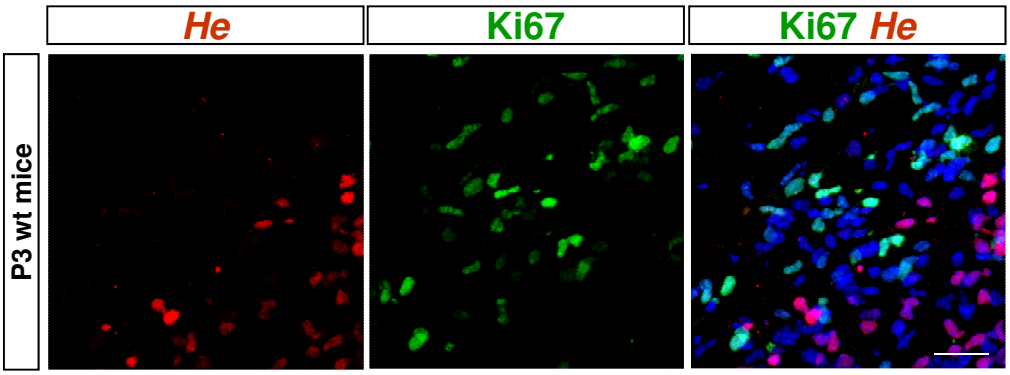

Figure S6. *He* is not expressed in proliferative cells at postnatal stages. Representative images at the GZ-MZ border of the ventro-medial striatum showing lack of co-localization between *He* and the proliferative marker Ki67 at P3. Scale bar: 20 µm.

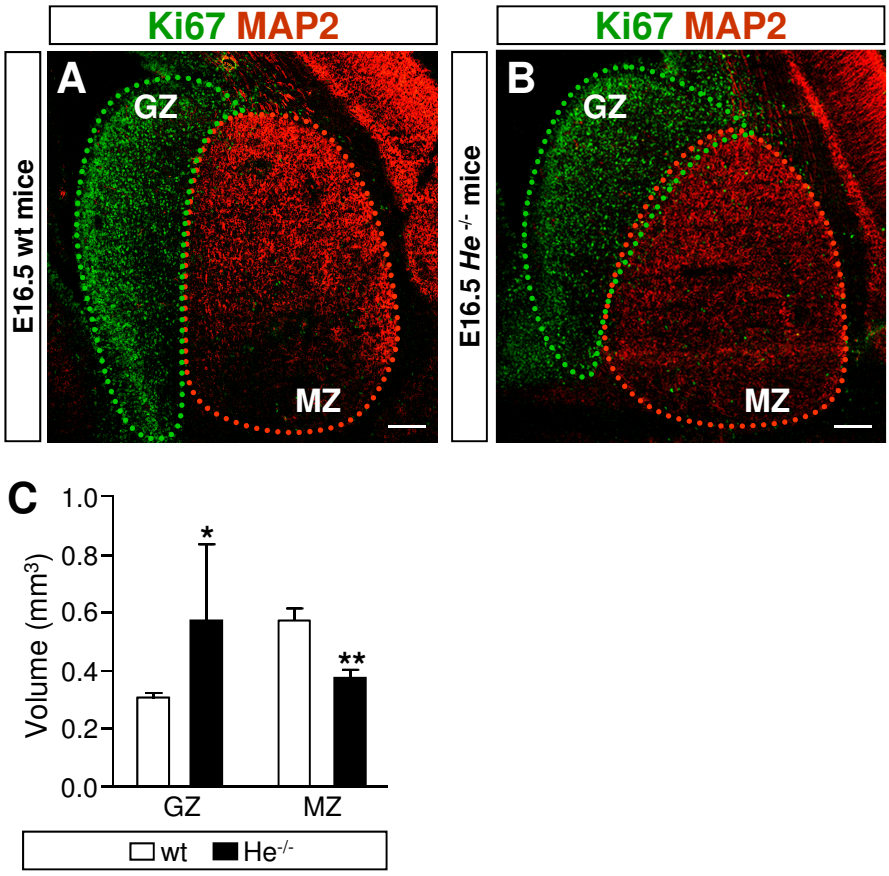

Figure S7. *He*$^{-/-}$ mice show an increase in the volume of the proliferative area. (**A-B**) Representative pictures of E16.5 striatal primordium double stained for Ki67 and MAP2 in wt and *He*$^{-/-}$ mice. Note the enlargement observed in the Ki67 positive proliferative zone of *He*$^{-/-}$ mice compared to wt mice. Proliferative and non-proliferative areas are delimited by dotted lines in green and red, respectively. Scale bar: 200 μm. (**C**) Quantification of the volume of GZ and MZ of wt and *He*$^{-/-}$ mice at E16.5. Results represent the mean ± s.e.m. of 4-6 mice per condition. Statistical analysis was performed using Student's t-test; *$p < 0.05$, **$p<0.005$.

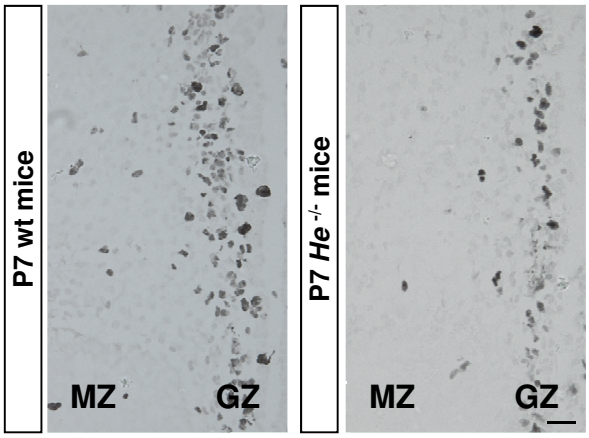

Figure S8. The number of proliferative progenitors in the GZ is reduced in the absence of *He* at P7. Representative photomicrographs of Ki67+ cells in the dorsal GZ of wt and *He*$^{-/-}$ mice at P7. Scale bar: 20 μm

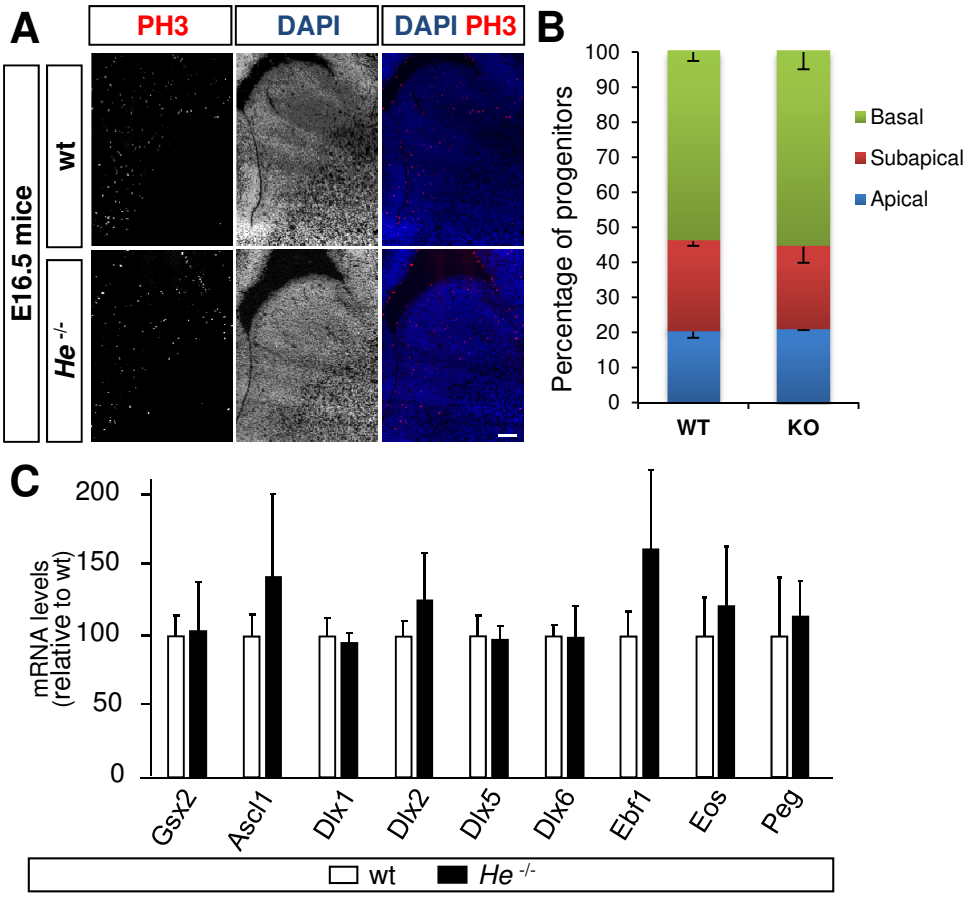

Figure S9. *He* does not affect radial glia subtypes. (**A-B**) Immunohistochemistry for PH3 in *He*$^{-/-}$ and wt striatal coronary sections at E16.5 and quantification of the percentage of basal, subapical and apical progenitors. Basal progenitors are predominant in the striatal GZ at E16.5 with no changes in the percentage between *He*$^{-/-}$ and wt conditions. Scale bar: 200 μm. Results represent the mean ± s.e.m. of 4-6 mice per condition. Statistical analysis was performed using Student's t-test; *p < 0.05, ***p<0.001. (**C**) We analyzed the levels of mRNA expression of several progenitor markers in the striatum of E16.5 wt and *He*$^{-/-}$ mice by Q-PCR. No differences are observed between genotypes. Results represent the mean ± s.e.m. of 4-5 LGEs from each genotype.

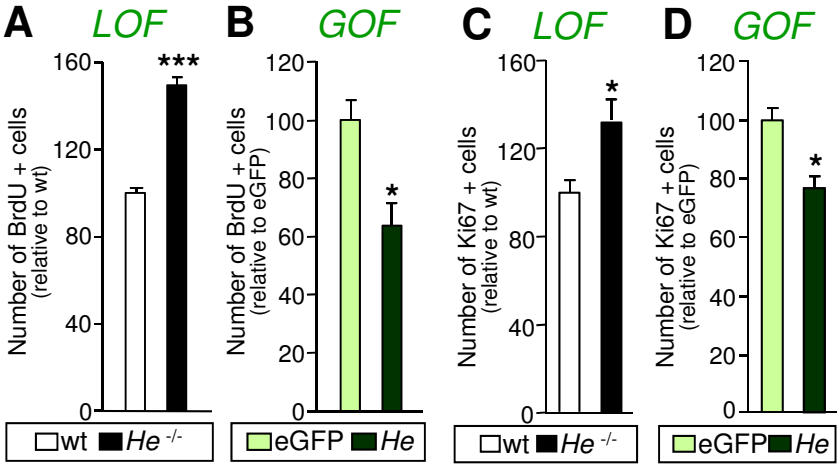

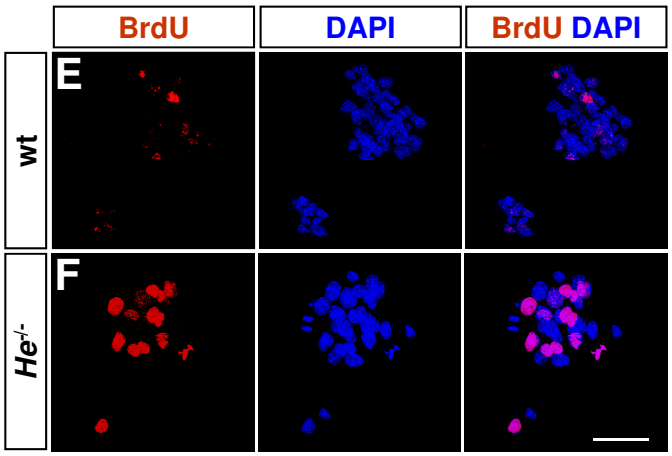

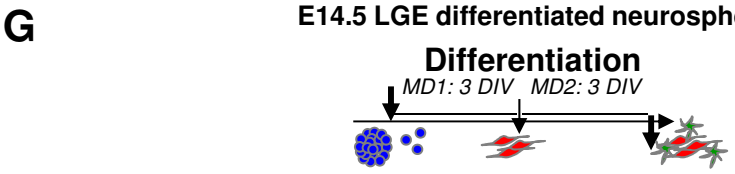

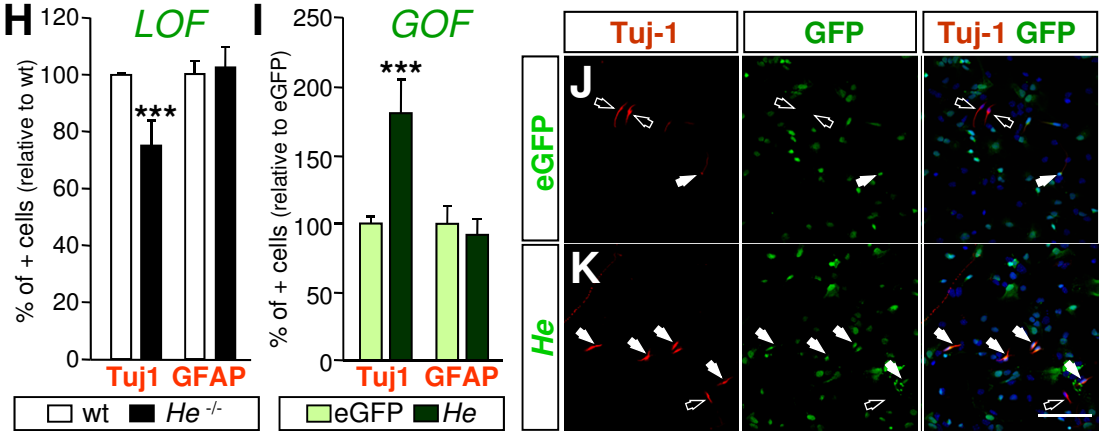

Figure S10. *He* regulates NPC proliferation and neurogenesis *in vitro.* (**A**) (**A**) Loss of function (*LOF*) experiments demonstrated that more NPCs incorporate BrdU in neurospheres derived from *He*$^{-/-}$ mice compared to wt mice. (**B**) Gain of function (*GOF*) experiments showed that *He* over-expression in wt neurospheres reduced the number of NPCs that incorporate BrdU compared to the control eGFP over-expression cultures. (**C**) *LOF* experiments demonstrated an increase in Ki67 positive proliferating cells in the absence of *He*. (**D**) *GOF* experiments showed that *He* over-expression reduced the number of Ki67-positive NPCs compared to neurosphere cultures over-expressing eGFP alone. (**E-F**) Representative images of BrdU incorporation in wt (**E**) and *He*$^{-/-}$ (**F**) mice derived neurospheres. Note the increase in the number of cells that are positive for BrdU in the *He*$^{-/-}$ NPCs. Scale bar: 50 μm. (**G**) Schematic timeline of the differentiation of E14.5 LGE derived neurospheres. (**H**) *LOF* experiments prove that *He* loss produced a significant reduction in the number of β-III-tubulin (Tuj-1)+ neurons without affecting the number of GFAP+ astrocytes. (**I**) *GOF* experiments show that *He* over-expression increased significantly the number of β-III-tubulin (Tuj-1)+ neurons but did not modify the number of GFAP+ astrocytes. (**J-K**) Representative photomicrographs of differentiated NSCs cultures over-expressing *He* (*He*) (**J**) or the control eGFP plasmid (**K**), double stained for eGFP and the neuronal differentiation marker β-III-tubulin (Tuj-1). White arrows point to double stained cells and open arrows point to single Tuj-1+ cells. Scale bar: 60 μm. Results represent the mean ± s.e.m. of 4-5 LGE-derived neurosphere cultures. Statistical analysis was performed using Student's t-test; *$p < 0.05$, ***$p < 0.001$.

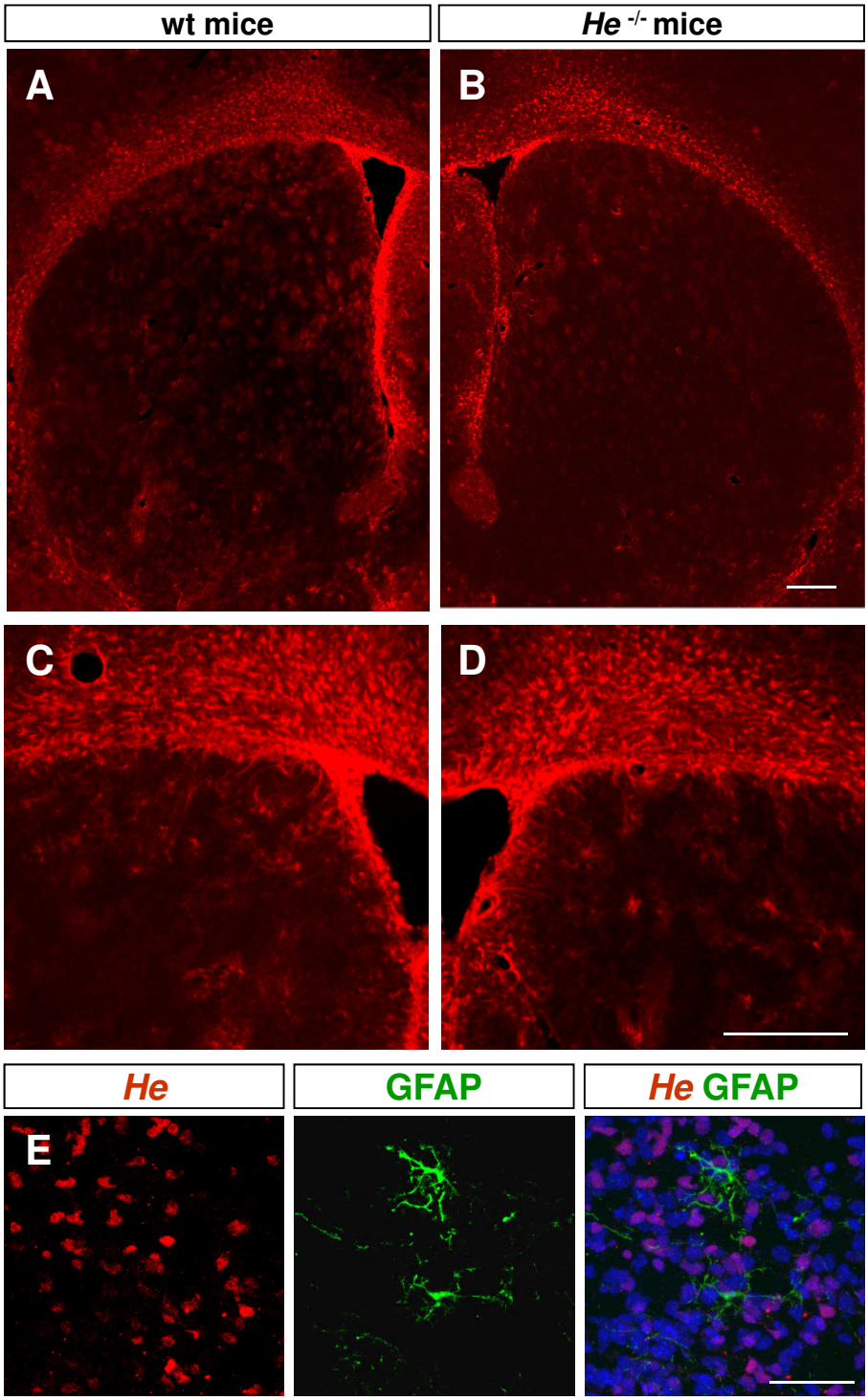

Figure S11. *He* is not involved in the generation of GFAP-positive astrocytes. (**A-D**) Striatal coronal sections immunostained for GFAP in wt (**A,C**) and *He*$^{-/-}$ adult mice (**B,D**) at low and high magnification (**A-B** and **C-D**, respectively). No differences are observed between the two genotypes. Scale bar: 200 μm. (**E)** Representative photomicrograph showing the lack of co-localization between *He* and the glial marker GFAP in a coronal dorsomedial striatal section at P3 Scale bar: 30 μm.

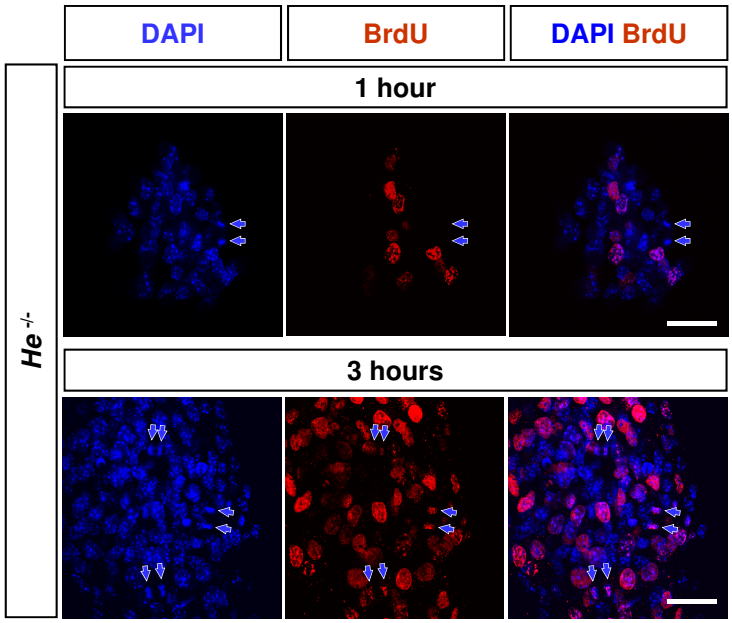

Figure S12. Analysis of the mitotic index. Representative image of BrdU and DAPI immunocytochemistry of neurospheres during the analysis of the mitotic BrdU labeling index. Note that after 1 hour almost all mitotic cells are negative for BrdU whereas after 3 hours almost all of them are positive. Double arrows indicate mitotic cells. Scale bar: 50 μm.

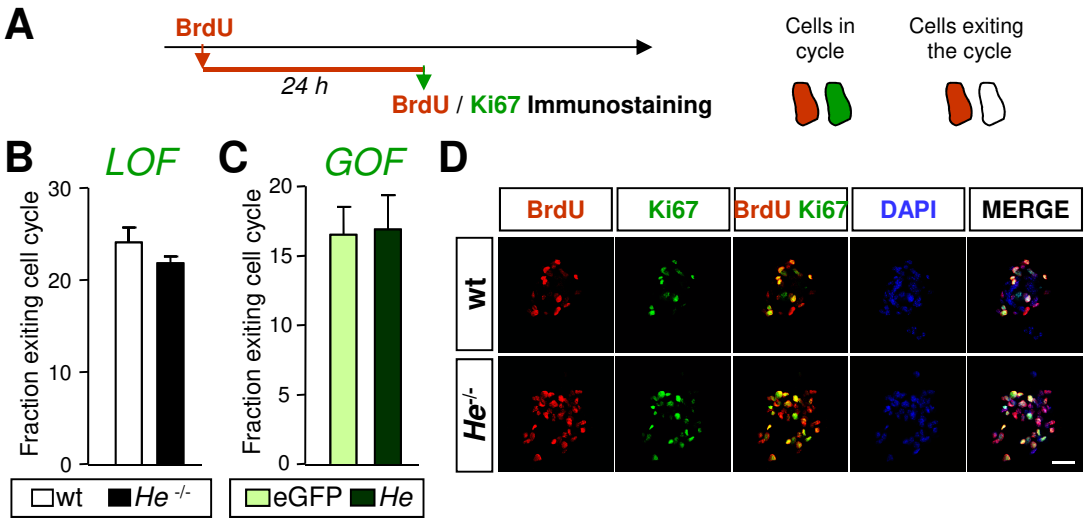

Figure S13. Helios does not affect the fraction of cells exiting the cell cycle. (**A**) Schematic timeline of cell cycle exit experiments in which double staining for BrdU and Ki67 was performed in NPCs cultures after a 24h pulse of BrdU. (**B**) *LOF* experiments showed no differences in cell cycle exit between *He*$^{-/-}$ and wt mice-derived neurospheres. (**C**) *GOF* experiments revealed that *He* over-expression does not produce changes in cell cycle exit. (**D**) Representative images showing no differences in cell cycle exit between wt and *He*$^{-/-}$ mice-derived neurospheres. Scale bar: 50 μm.

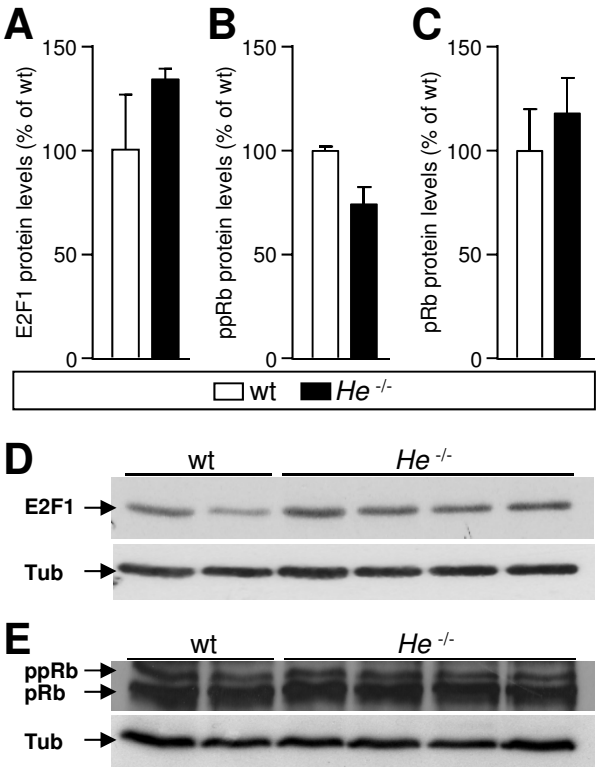

Figure S14. He does not regulate the levels of E2F1 or hyper or hypo-phosphorylated retinoblastoma (Rb). (**A**) Lack of differences in the levels of E2F1 between wt and *He*$^{-/-}$ mice. (**B-C**) Similarly, the levels of hyper-phosphorylated Retinoblastoma (ppRb; **B**) or hypo-phosphorylated Retinoblastoma (pRb; **C**) do not show differences between phenotypes. Results represent the mean ± s.e.m. of 4-5 LGE-derived neurosphere cultures. Statistical analysis was performed using Student's t-test. (**D**) Representative bands of E2F1 in wt and *He*$^{-/-}$ mice. (**E**) Representative bands of ppRb and pRb in wt and *He*$^{-/-}$ mice. Tub; tubulin.

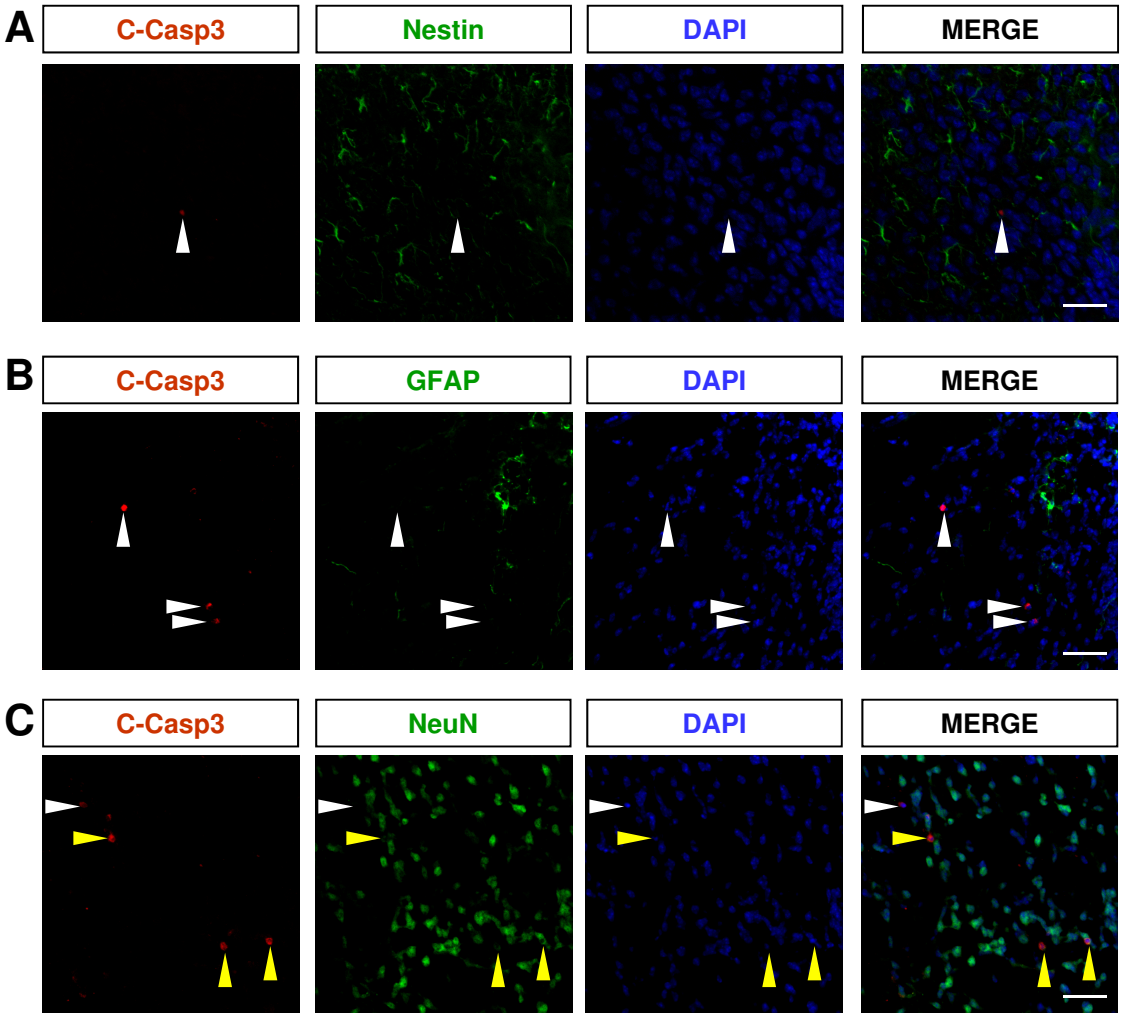

Figure S15. Cell death induced by *He* loss is detected in neurons but not in NPCs or glial cells. (**A**) Representative photomicrographs of striatal P3 coronal sections showing a lack of co-localization of Nestin and cleaved caspase 3 (C-casp3) in the dorsal striatum. White arrowheads point to C-casp3 single labeled cells. Scale bar: 30 μm. (**B**) Representative photomicrographs of striatal P3 coronal sections showing lack of co-localization of GFAP and cleaved caspase 3 (C-casp3) in the dorsal striatum. White arrowheads point to C-casp3 single labeled cells. Scale bar: 30 μm. (**C**) Representative photomicrographs of striatal P3 coronal sections showing co-localization of NeuN and cleaved caspase 3 (C-casp3) in the dorsal striatum. White arrowheads point to C-casp3 single labeled cells. Yellow arrowheads point to C-casp3 and NeuN double labeled cells. Scale bar: 30 μm.

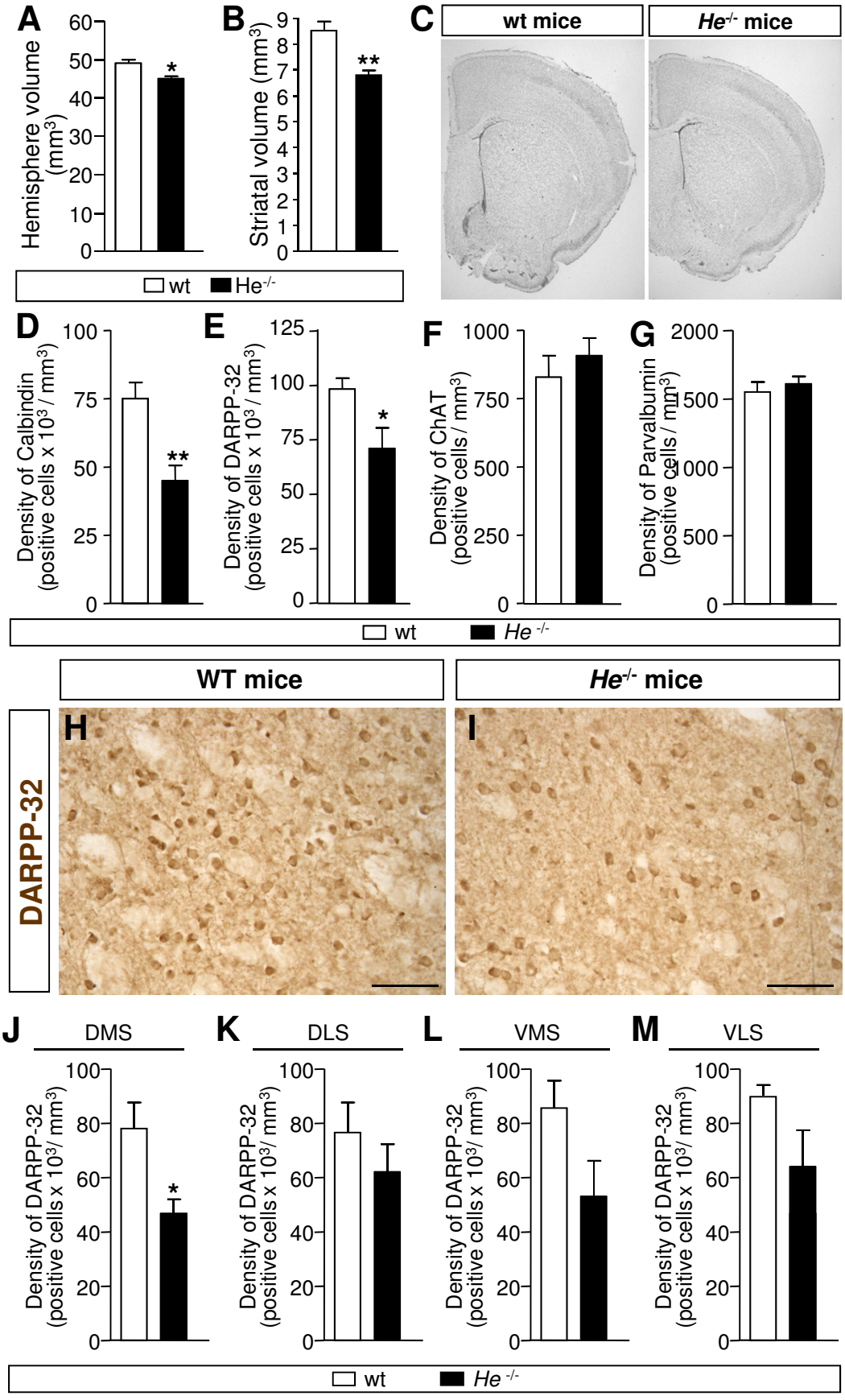

Figure S16. *He* loss produces a decrease of MSN density at the DMS. (**A,C**) Brain hemisphere volume was slightly reduced in *He*$^{-/-}$ mice compared to wt mice. (**B,C**) Striatal volume was significantly reduced in approximately a 20% in *He*$^{-/-}$ mice compared to wt mice. (**C**) Representative photomicrographs of cresyl violet staining of wt and *He*$^{-/-}$ mice brains showing the reduction in striatal volume. (**D**) Density of striatal calbindin+ cells is reduced in *He*$^{-/-}$ adult mice compared to wt adult mice. (**E**) Density of striatal DARPP-32+ cells is reduced in *He*$^{-/-}$ adult mice compared to wt adult mice. (**F**) The density of striatal ChAT+ cells is not altered between wt and *He*$^{-/-}$ adult mice. (**G**) The density of striatal Parvalbumin+ cells is not altered between wt and *He*$^{-/-}$ adult mice. (**H-I**) Representative photomicrographs of DARPP-32 immunohistochemistry in the dorsomedial striatum of wt (**H**) and *He*$^{-/-}$ (**I**) mice. Scale bar: 50 µm. (**J-M**) Density of striatal DARPP-32+ cells is specifically reduced in the DMS (**J**) in *He*$^{-/-}$ adult mice compared to wt adult mice. No differences are found in the DLS (**K**), VMS (**L**) and VLS (**M**) between both genotypes**.** DMS, dorsomedial striatum; DLS, dorsolateral striatum; VMS, ventromedial striatum; VLS, ventrolateral striatum.

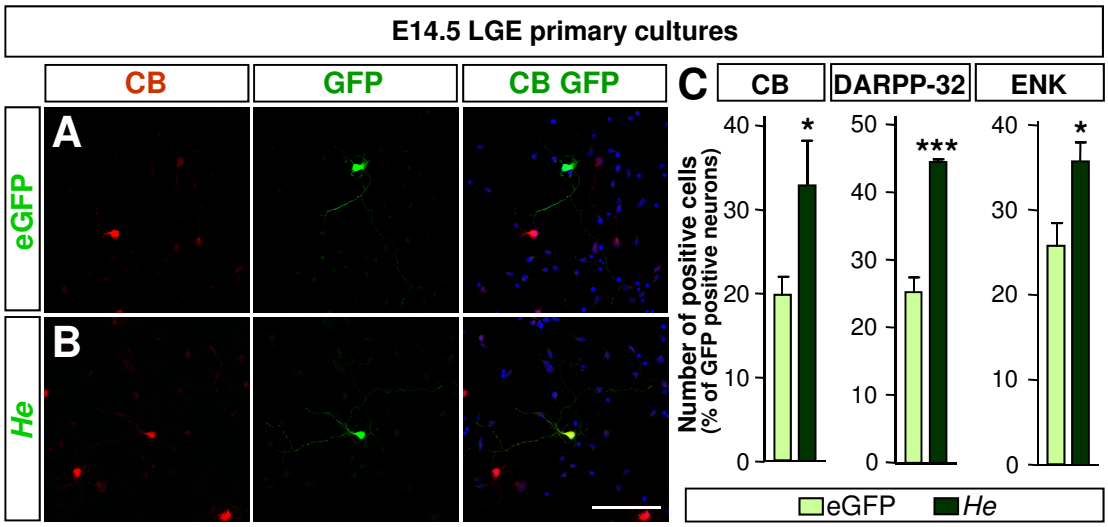

Figure S17. *He* induces a striatal MSN phenotype. (**A-B**) Representative photomicrographs showing double immunocytochemistry for eGFP and calbindin (CB) in primary striatal cultures overexpressing eGFP alone (**A**) or eGFP-*He* (*He*) (**B**). (**C**) Quantification of the number of *He* and eGFP positive cells co-localizing with CB, DARPP-32 and ENK. The bars in the graph represent the percentage of transfected cells positive for each marker out of the total number of transfected eGFP-positive cells. Scale bar: 50 μm. Results represent the mean ± s.e.m. of 4-5 LGE- primary cultures. Statistical analysis was performed using Student's *t*-test; *p < 0.05, ***p < 0.001.

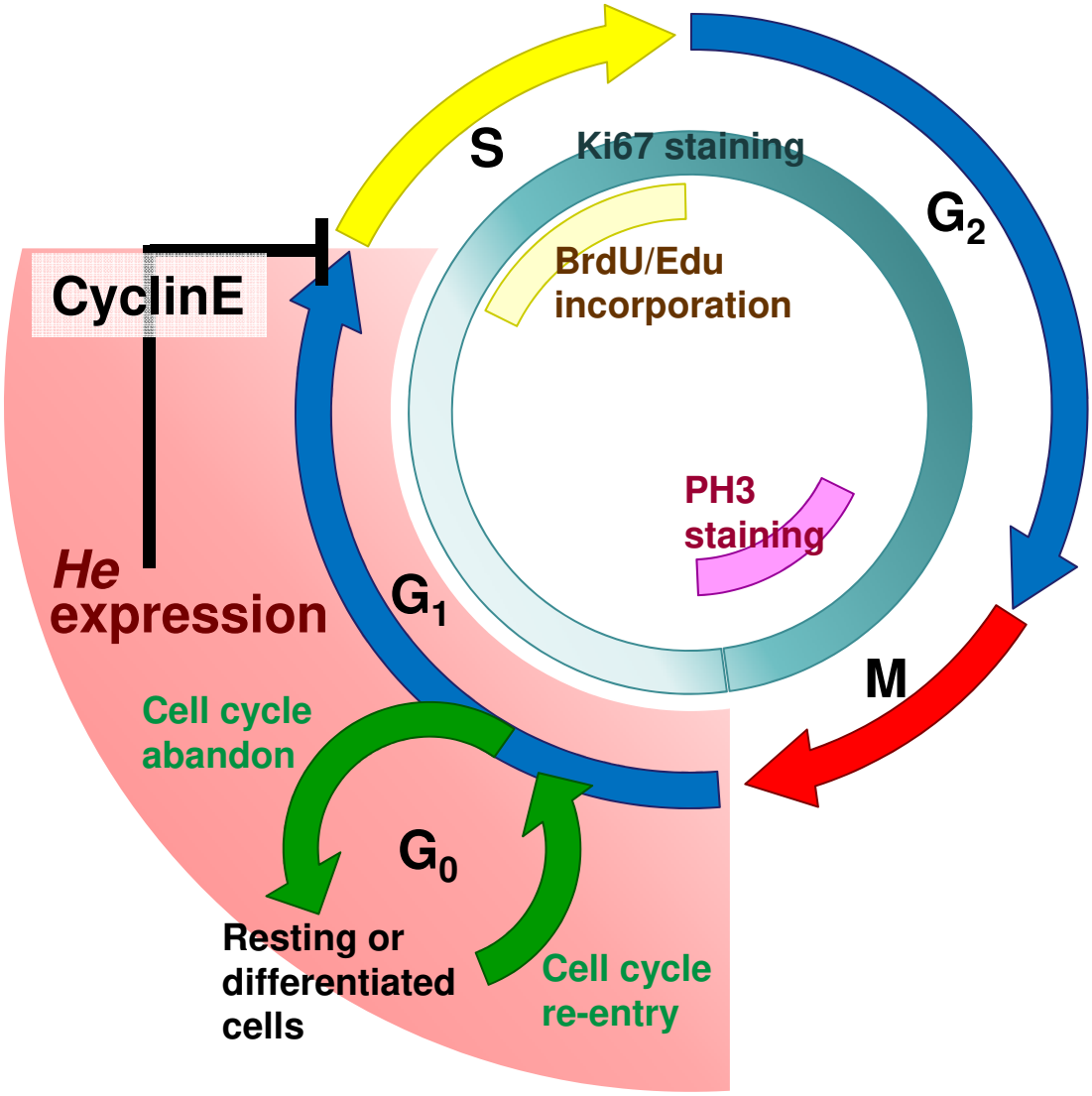

Figure S18. Schematic representation of He expression along NPCs cell cycle. Cell cycle phases are shown in different colors; G_0, green; G_1 blue; S, yellow; G_2, blue; and M, red. Inside circle and semicircles show the levels of Ki67 through cell cycle phases. Note that Ki67 immunostaining labels all phases except G_0 and the levels of expression are lower in phase G_1 (light blue); BrdU incorporation that labels S phase is represented in light yellow; and PH3 immunostaining that labels M phase in pink. Cells entering the phase G_0 abandon the cell cycle and become resting cells or postmitotic differentiated cells. However, resting cells can re-enter into the cell cycle. *He* is expressed in G_0 differentiated neurons and G_1 NPCs. In the later this transcription factor decrease Cyclin E to impair G_1-S phase transition and induce NPCs neuronal differentiation.